Naval Research Laboratory
Washington, DC 20375-5320

NRL/MR/6180--04-8765

Fire and Smoke Simulator (FSSIM) Version 1 – Theory Manual

JASON E. FLOYD
SEAN P. HUNT

Hughes Associates, Inc.
Baltimore, MD

FREDERICK W. WILLIAMS

Navy Technology Center for Safety and Survivability
Chemistry Division

PATRICIA A. TATEM

ITT Industries Advanced Engineering and Sciences Division
Alexandria, VA

March 31, 2004

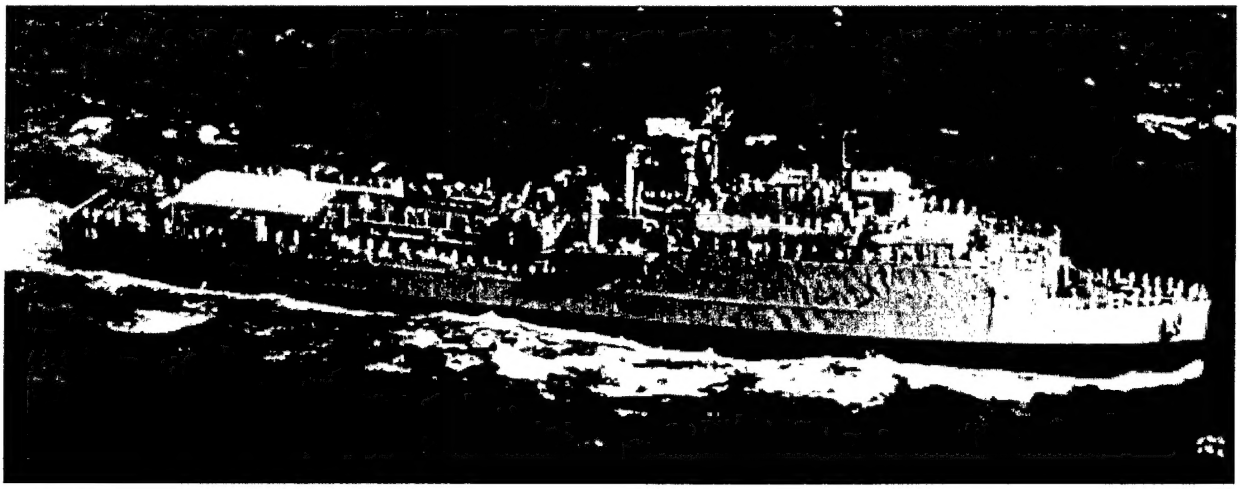

REPORT DOCUMENTATION PAGE

Form Approved
OMB No. 0704-0188

1. REPORT DATE *(DD-MM-YYYY)*	2. REPORT TYPE	3. DATES COVERED *(From - To)*
March 31, 2004	Memorandum Report	2003

4. TITLE AND SUBTITLE

Fire and Smoke Simulator (FSSIM) Version 1 – Theory Manual

5a. CONTRACT NUMBER

5b. GRANT NUMBER

5c. PROGRAM ELEMENT NUMBER

6. AUTHOR(S)

Jason E. Floyd,* Sean P. Hunt,* Frederick W. Williams, and Patricia A. Tatem†

5d. PROJECT NUMBER

5e. TASK NUMBER

5f. WORK UNIT NUMBER

7. PERFORMING ORGANIZATION NAME(S) AND ADDRESS(ES)

Naval Research Laboratory, Code 6180
4555 Overlook Avenue, SW
Washington, DC 20375-5320

8. PERFORMING ORGANIZATION REPORT NUMBER

NRL/MR/6180--04-8765

9. SPONSORING / MONITORING AGENCY NAME(S) AND ADDRESS(ES)

Office of Naval Research
800 North Quincy Street
Arlington, VA 22217-5660

10. SPONSOR / MONITOR'S ACRONYM(S)

11. SPONSOR / MONITOR'S REPORT NUMBER(S)

12. DISTRIBUTION / AVAILABILITY STATEMENT

Approved for public release; distribution is unlimited.

13. SUPPLEMENTARY NOTES

*Hughes Associates, Inc., 3610 Commerce Drive, Baltimore, MD
†ITT Industries Advanced Engineering and Sciences Division, Alexandria, VA

14. ABSTRACT

There currently exists a number of computational tools for examining the effects of a fire that can be applied to a ship and its crew. One could use hand calculations for examining simple scenarios in single compartments. Simple rules can be used to extend this approach to multiple compartments. Zone models are suitable for examining somewhat more complex, time-dependent scenarios involving multiple compartments and levels, but stability can be a problem for multi-level scenarios with Heating, Ventilation, and Air Conditioning (HVAC) systems, and for post-flashover conditions. Computational fluid dynamics (CFD) models can yield detailed information about temperatures, heat fluxes, and species concentrations; however, the time penalty of this approach currently makes using CFD unfeasible for long periods of real time or large computational domains. There is another class of models that have traditionally played supporting roles in fire modeling. This class is constituted by a variety of network models, which are used for ventilation systems in buildings or fluid flow in piping networks. These models, however, lack specific physics required for fire modeling. To meet the computational speed and algorithm requirements, it was decided to develop Fire and Smoke Simulator (FSSIM) as a network fire model. This document (Theory Manual) describes the equations solved, and the solution algorithm for the heat and mass transfer along with the equations and algorithms for FSSIM sub-models.

15. SUBJECT TERMS

Fire; Network; Model; Simulation

16. SECURITY CLASSIFICATION OF:			17. LIMITATION OF ABSTRACT	18. NUMBER OF PAGES	19a. NAME OF RESPONSIBLE PERSON
a. REPORT	b. ABSTRACT	c. THIS PAGE			Frederick W. Williams
Unclassified	Unclassified	Unclassified	UL	43	19b. TELEPHONE NUMBER *(include area code)* 202-767-2476

Standard Form 298 (Rev. 8-98)
Prescribed by ANSI Std. Z39.18

CONTENTS

FIRE AND SMOKE SIMULATOR (FSSIM)
VERSION 1 – THEORY MANUAL

1.1 Background

In both peacetime and during war, fire represents a significant threat to any ship. A fire, whether started by a mechanical failure, intentional or unintentional human actions, or damage from a weapon hit, threatens the ship in a number of ways. The crew's health and ability to operate the ship is affected by direct exposure to the fire or by the spread of smoke and toxic gasses through the ship by either natural or mechanical ventilation. Electrical systems can be degraded by thermal exposure, exposure to acid gasses in the combustion products, or by electrical failure resulting from soot deposition, which might include hampered cooling or dielectric breakdown from the electrical conductivity of the soot. Mechanical systems can suffer thermal damage. Lastly, fire growth and spread could potentially ignite explosive materials, rocket motors, aviation fuel, or other highly flammable substances, which could possibly result in temperatures or overpressures high enough to affect the ship structurally.

There currently exist a number of computational tools for examining the effects of a fire that can be applied to a ship and its crew. One could use hand calculations for examining simple scenarios in single compartments. Simple rules can be used to extend this approach to multiple compartments. Zone models are suitable for examining somewhat more complex, time-dependent scenarios involving multiple compartments and levels, but stability can be a problem for multi-level scenarios, scenarios with Heating, Ventilation, and Air Conditioning (HVAC) systems, and for post-flashover conditions. Computational fluid dynamics (CFD) models can yield detailed information about temperatures, heat fluxes, and species concentrations; however, the time penalty of this approach currently makes using CFD unfeasible for long periods of real time or large computational domains. There is another class of models which have traditionally played supporting roles in fire modeling. This class is constituted by a variety of network models, which are used for ventilation systems in buildings or fluid flow in piping networks. These models, however, lack specific physics required for fire modeling.

The need for fire modeling occurs through the "cradle-to-grave" lifetime of a ship, which encompasses the phases of concept design, detailed design and hazards evaluation, doctrine and tactics development, ship operation and maintenance, and crew training. In the concept design phase, fire modeling is needed to evaluate ship designs and design philosophies in order to quickly arrive at an overall concept to meet required performance goals. As this concept is refined into a detailed design, fire modeling is continued to evaluate ship vulnerability and recoverability and to begin the process of defining ship operation. Both of these phases could

Manuscript approved March 4, 2004.

potentially require evaluating the fire behavior of a ship and its system for hundreds of scenarios in design cycles spanning a few months time. Doctrine and tactics planning also require evaluating many separate fire scenarios in combination with a number of candidate doctrines. During the operational phase of a ship's lifetime fire modeling can support crew training through interactive training simulations. Fire modeling can also aid in the recovery from a fire event by providing a faster than real time predictive capability to gauge the potential effectiveness of a course of action.

For each of the aforementioned uses of fire modeling, speed and the ability to model large complexly interconnected spaces with ventilation, detection, and suppression with a reasonable degree of accuracy are performance requirements for the model. Hand calculations, while fast, have limitations in applicability and large uncertainties in their results. CFD computations have the potential to be accurate to any desired degree, but are slow. Zone models balance well computational time and accuracy; however, in general these models do not perform well with ventilation systems and they lack the ability to model control systems. To meet the computational speed and algorithm requirements, it was decided to develop Fire and Smoke Simulator (FSSIM) as a network fire model.

1.2 Network Model Overview

A network model represents a one-dimensional abstraction of the physical world. The prototype being modeled is represented by a set of nodes and node connections, where the nodes contain one set of physical variables and the node connections represent transfers of those variables between nodes. Contrast this with a zone model which uses two sets of variables or a CFD model which uses a multitude. A network representation allows for maximum physical extent of a simulation with a minimum set of equations, one per geometric volume of interest. Since the number of locations being solved for is kept to a minimum, a network model also has the potential for the faster execution speeds.

There are currently a number of network models in existence that are used for safety related simulations. Some of these include:

- TRAC – Transient Reactor Analysis Code. Used for simulating normal and accident conditions of nuclear power plant cooling systems (Spore, et al., 2000).
- RELAP – Reactor Excursion and Leak Analysis Program. Used for simulating normal and accident conditions of nuclear power plant cooling systems (USNRC, 2001).
- GOTHIC – Generation of Thermal Hydraulic Information for Containments. Used for simulating normal and accident conditions of nuclear power plant containment buildings and reactor buildings (George, et al., 2000a-b).
- MELCOR – Used for simulating normal and accident conditions of nuclear power plant containment buildings and reactor buildings including aerosol dispersion, core melt/core melt interactions, and hydrogen combustion (Gauntt, et al., 2000).
- CONTAM – Used for simulating the dispersal of airborne contaminants through a building and its associated HVAC systems (Dols, Walton, and Denton, 2000).

- COCOSYS – COntainment COdeSYStems Used for simulating accident conditions in light water nuclear power plant containment buildings and reactor buildings (Allelein *et al.*, 1999; Klein-Heβling *et al.*, 2000).

1.3 FSSIMv1.0 Overview

FSSIM is a network fire model written to simulate the spread of fire and smoke in a naval vessel. However, there is nothing in the model to preclude its use for other types of compartmented structures such as a building. FSSIM is written in standard Fortran 95 (Adams, et al., 1997) and as such is capable of being compiled on any platform for which a Fortran 95 compiler is available. In FSSIM each compartment in a structure is represented as a single node with surfaces (e.g. bulkheads, decks, and overheads) and vent openings (e.g. doors, hatches, etc.) represented as node connections. There is no practical limit ($2x10^9$ items of any type) to the size of an FSSIM simulation other than available computational resources and time.

FSSIMv1.0 has the following capabilities:

- 1D flow model including friction losses and temperature-dependent specific heat.
- 1D multiple-layer, temperature-dependent heat transfer.
- N-surface, gray-gas radiation heat transfer, including radiation streaming through openings.
- Bidirectional flow through horizontal (hatches) and vertical (doors) flow connections.
- Combustion product species tracking.
- Oxygen and fuel limited combustion.
- Multiple user-defined fires along with fire spread via compartment-to-compartment heat transfer.
- HVAC systems including ducts, dampers, and fans with forward and reverse flow losses and multiple fan models.
- Fire detection via heat, smoke, and fire detection
- Fire spread by compartment-specific criteria.
- Fire suppression via sprinklers, water mist, gaseous agents, aerosol agents, and foam.
- Fire spread prevention via boundary cooling.
- Simple control systems to link operation of equipment to sensors or times.
- Fast, near-real-time execution speed.

1.4 Documentation Overview

FSSIM documentation consists of three volumes. The FSSIM Theory Manual (this document), the FSSIM Users' Manual (Floyd, et al., 2004), and the FSSIM Validation Manual (Floyd, et al., 2004). The Theory Manual describes the equations solved, and the solution algorithm for the heat and mass transfer along with the equations and algorithms for FSSIM submodels. The Users' manual discusses creation of FSSIM input files including guidance in transforming a prototype structure to a network representation and explains the available outputs. Lastly, the Validation Manual documents FSSIM performance as compared to experimental data and other fire models.

There is a companion viewer for FSSIM called [MSU GUI NAME] that is under development by Mississippi State University. This viewer will display animated results of FSSIM calculations in a 3D representation of the ship (Haupt, et al., 2004).Hydraulic Solver

2.0 HYDRAULIC SOLVER

2.1 Overview

FSSIM uses a network or lumped-parameter approach to solve the time-dependent flow of gases through a series of vent-connected compartments and associated ventilation systems. In this approach, compartments are considered one dimensional, that is the pressure, mass, and energy content of a compartment are represented by one set of integral quantities. Flows through vents can be bi-directional in the sense of simultaneous inflow and outflow, but vector flow quantities, such as absolute flow direction, are not tracked. Ventilation systems are broken down in the simplest possible duct-node representation. Flow in ducts is assumed to be unidirectional. A duct is any length of ducting with bends, expansions, contractions, etc., where only one flow possibility exists. A node is typically a duct terminal, which can be either a compartment or a ventilation component joining multiple ducts such as a manifold or a tee. Figure 1 shows a simple compartment layout and its network representation.

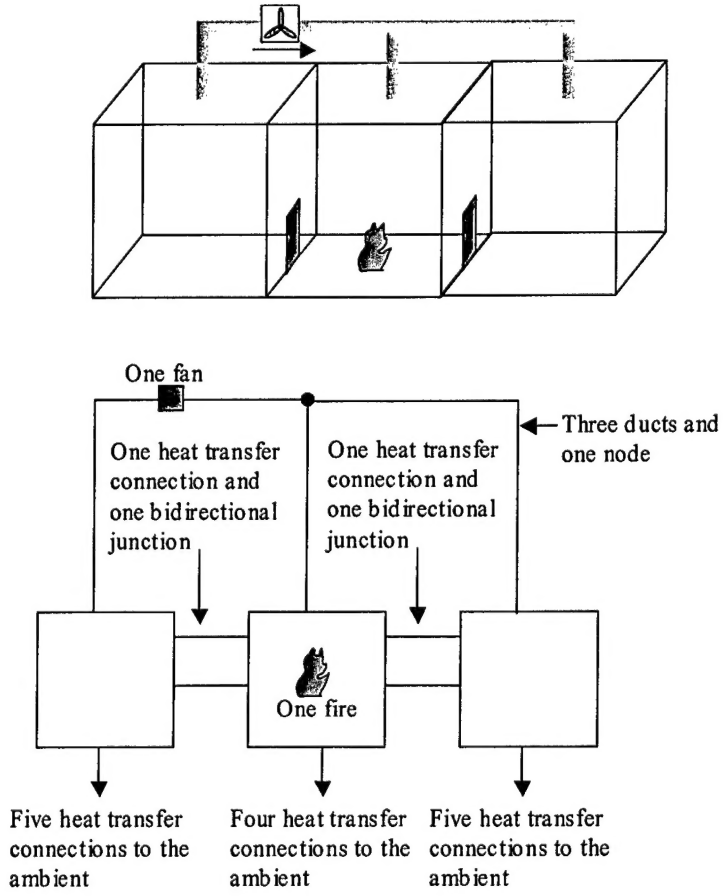

Figure 1: Network Model Concept

2.2 Conservation Equations in Derivative Form

The FSSIM hydraulic solver solves the 1D conservation equations for mass, momentum and energy. Energy and mass are conserved explicitly, whereas momentum is conserved implicitly. Energy and mass conservation use a control-volume approach, where the control volume is either a single compartment or a ventilation system node. Momentum is implicitly solved for at vent connections or in ducts. The set of equations used is taken from MELCOR (Gauntt, et al., 2000) with the removal of multiphase (condensable vapor, droplet, liquid pools, and bubbles) and interphase (phase-related drag and phase change) terms.

Mass Equation:

$$\frac{dM_i}{dt} = \sum_j \sigma_{ij} \rho_j^d v_j F_j A_j + \dot{M}_i \tag{1}$$

In this equation i is the control volume (compartment or duct node) j is a flow connection, d is a donor or upstream quantity, M is the total mass in a volume, A is flow area, F is a function that modifies the flow area (allows for opening/closing), σ is a flow direction and is +1 for flow out of i and –1 for flow into i, v is the velocity, and ρ is the density. The mass source term, $\dot{M}_i$, represents mass additions due to pyrolysis and suppression. The change in mass over time is equal to the net flow into the volume plus the net source/sink of mass in the volume. For a duct node, there is no mass storage or source term, so a modified equation can be given:

$$0 = \sum_j \sigma_{ij} \rho_j^d v_j F_j A_j \tag{2}$$

Energy Equation:

$$\frac{dE_i}{dt} = \sum_j \sigma_{ij} v_j F_j A_j \rho_j^d h_j^d + \dot{E}_i \tag{3}$$

In this equation, variable definitions are as above with the addition of E for the energy content of the volume, and h is a species enthalpy. As with mass, duct nodes do not store energy. The energy source term, $\dot{E}_i$,represents the addition or removal of energy due to combustion heat release, heat removal due to suppression, heat transfer to surfaces, and enthalpy changes due to mass changes resulting from pyrolysis, suppression, and compartment vent flows.

Momentum Equation:

$$\rho_j L_j \frac{dv_j}{dt} = (P_i - P_k) + (\rho g \Delta z)_j + \Delta P_j - \frac{1}{2} K_j \rho_j |v_j| v_j \tag{4}$$

Additional variables in this equation are k for a control volume, P for a control volume pressure, ΔP for a momentum source term such as a fan, K for flow losses resulting from wall friction and form losses (e.g. fittings, flow obstructions, area changes, and entrances/exits),

($\rho g \Delta z$) for buoyancy head, and L for the momentum length of the flow connection. Buoyancy head and momentum length will be discussed later. Note that the above momentum equation does not contain a term for kinetic energy. This term is impractical to define for a lumped parameter model, and in general its omission is a minor source of error (Gauntt, et al., 2000)

In general, this set of equations must be solved in an iterative manner due to the stiffness of the pressure-velocity coupling. There may be flow connections whose velocities oscillate direction during this iterative process. To aid in convergence an iteration-dependent donor formulation is used. In the momentum equation the density term is modified as follows:

$$\rho_j^{n+1} = \beta\rho_j^n + (1-\beta)\rho_d \tag{5}$$

The density used in the momentum equation at inner loop iteration n+1, see 2.6.2, is a linear combination of the density used for iteration n and the donor or upstream density. β ranges from 0 to 1. For the first third of the iterations β=0 and a pure upstream density is used. For the last third of the iterations β =1 and the prior iteration density is used. β varies linearly from 0 to 1 over the middle third of the iterations. If flow reversal is occurring, then it is possible that the density being used in the momentum equation will be varying greatly between iterations. This can result in an oscillation. By allowing the density term to vary from the upwind donor density to a fixed donor density, large changes in the new velocity solution are reduced. In this manner the negative impact of oscillating flows on convergence can be minimized. This donor approach is only used for the momentum equation; the mass and energy equations always use the upstream density. Thus, while this approach may result in errors in the velocity prediction, it will not impact the overall mass and energy conservation.

Along with the conservation equations, an equation of state is also required. This is given by

$$P_i V_i = \frac{R}{mw_{air}} \frac{E_i}{c_{p_i}(T_i)} \tag{6}$$

In the above equation, c_p is the specific heat of the compartment at its current temperature, mw_{air} is the molecular weight of air, and R is the real gas constant.

2.3 Conservation Equations in Difference Form

Equations 1, 3, and 4 are expressed in finite difference form for solution. The mass and energy equations are expressed using an end-of-time step explicit Euler difference scheme. The momentum equation is expressed in a semi-implicit form. The result is that mass and energy will be conserved absolutely; however, momentum will not be absolutely conserved.

Mass Equation:

$$M_i^n = \left(\sum_j \sigma_{ij} \rho_j^d v_j^n F_j^n A_j + \dot{M}_i^n \right) \Delta t^n + M_i^{n-1} \tag{7}$$

In the above equation n indicates the current time step number and n-1 the prior time step with $\Delta t^n = t^n - t^{n-1}$.

Energy Equation:

$$E_i^n = \left(\sum_j \sigma_{ij} v_j^n F_j^n A_j \rho_j^d h_j^d + \dot{E}_i^n \right) \Delta t^n + E_i^{n-1} \tag{8}$$

Momentum Equation:

$$v_j^n = v_j^{n-1} + \frac{\Delta t^n}{\rho_j L_j} \left(\tilde{P}_i^n - \tilde{P}_k^n + \Delta P_j + (\rho g \Delta z)_j^{n-1} \right) - \frac{K_j \Delta t^n}{2L_j} \left(v_j^{n-} - v^{n+} \left| v_j^n \right| - \left| v_j^{n+} \right| v_j^{n-} \right) \tag{9}$$

In the above equation n- indicates the previous iteration, n+ indicates a next time step gases, and ~ indicates a linearized prediction. In the friction term, the velocity at the next time step is approximated with a tangent/secant approach. The n+ value is the velocity from the prior iteration if the velocity direction did not change during iterations, and it is zero if the velocity changed during iterations.

The ~ values for the pressure indicate an approximation of the next time step pressure based on the next time step velocities. This approximation accounts for the change in pressure resulting from energy inputs into the control volume from either sources and sinks such as fires and wall heat transfer, or from inputs and outputs due to mass flow in flow connections.

$$\tilde{P}_i^n = P_i^{n-1} + \frac{dP_i^{n+}}{dE_i^n} \frac{dE_i^n}{dt} \Delta t^n \tag{10}$$

$$\frac{dE_i^n}{dt} = \dot{E}_i^n + \sum_j \sigma_j \rho_j^d F_j^n A_j v_j^n h_j^d \tag{11}$$

$$\frac{dP_i^{n+}}{dE} = \frac{R}{V_i m w_{air}} \frac{1}{c_{p_i}^{n+}} \tag{12}$$

$$\tilde{P}_i^n = P_i^{n-1} \frac{c_{p_i}^{n-}}{c_{p_i}^{n+}} + \frac{R}{m w_{air} V_i} \frac{1}{c_{p_i}^{n+}} \frac{dE_i^n}{dt} \Delta t^n \tag{13}$$

where I is any control volume.

Ideally, we want to use the new specific heat in determining the pressures change. However, that involves knowing all the mass flows in and out of the volume. To avoid making the solution matrix overly large, the new compartment specific heat can be estimated based on the prior time

step velocities. As the velocity solution converges, the specific heat solution will converge as well. Since the specific heat of air is weakly varying with temperature, as long as the velocity and resulting temperature change in a compartment are limited by the time step size, the lag in specific heat convergence will have a minimal impact on the solution. Since the linearized pressure is being computed based on an energy derivative, in order to conserve energy the old pressure must be multiplied by the ratio of old to predicted specific heats in Equation 13. Once the extrapolated pressures are computed, the momentum equation becomes:

$$
\begin{aligned}
&v_j^n\left(1+\frac{K_j\Delta t^n}{2L_j}\left|v_j^{n-}-v^{n+}\right|\right)-\frac{\Delta t^{n^2}}{\rho_j L_j}\frac{R}{mw_{air}}\\
&\left(\frac{1}{V_i c_{p_i}^{\,n+}}\sum_{j1\text{ connected to }i}\sigma_{j1}\rho_{j1}^d A_{j1}F_{j1}^n v_{j1}^n h_{j1}^d-\frac{1}{V_k c_{p_k}^{\,n+}}\sum_{j2\text{ connected to }k}\sigma_{j2}\rho_{j2}^d A_{j2}F_{j2}^n v_{j2}^n h_{j2}^d\right)=\\
&v_j^{n-1}+\frac{\Delta t^n}{\rho_j L_j}\left(P_i^{n-1}\frac{c_{p_i}^{\,n-}}{c_{p_i}^{\,n+}}+\dot q_i\frac{R}{mw_{air}V_i c_{p_i}^{\,n+}}-P_k^{n-1}\frac{c_{p_k}^{\,n-}}{c_{p_k}^{\,n+}}-\dot q_k\frac{R}{mw_{air}V_k c_{p_k}^{\,n+}}+\Delta P_j+(\rho g\Delta z)_j^{n-1}\right)\\
&+\frac{K_j\Delta t^n}{2L_j}\left(v_j^{n+}\left|v_j^{n-}\right.\right)
\end{aligned}
\tag{14}
$$

In the case of a duct node the critical equation is the conservation of mass since mass is not stored in ducts. Therefore, for a duct node, Equation 7 is solved if it is an internal node that connects multiple ducts. For an external duct node, one that connects a duct to a compartment, the node pressure is the same as the compartment pressure; therefore, external node pressure is not a solution variable. Thus when Equation 9 is used for a duct, the $\tilde{P}^n$'s will be replaced by a P^n for each internal node.

2.4 Hydraulic Submodels

2.4.1 Energy Source Term

The $\dot{E}_i^n$ term in Equation 8 is composed of a number of energy sources and sinks. This term is given by:

$$\dot{E}_i^n=\dot q_f(1-\chi_f)-\dot q_{f,pyro}+\dot m_{f,pyro}h_{f,pyro}-\dot q_{i,supp}+\dot m_{i,supp}h_{i,supp}+\dot q_{i,gas}-\sum_w\dot q_{i,w,c} \tag{15}$$

where $\dot q_f(1-\chi_f)$ is the convective heat release, $\dot q_{f,pyro}$ is the heat of pyrolysis of the fuel, $\dot m_{f,pyro}h_{f,pyro}$ is the enthalpy of the pyrolyzed fuel, $\dot q_{i,supp}$ is the energy removal due to suppression (e.g. water evaporation), $\dot m_{i,supp}h_{i,supp}$ is the enthalpy of the suppression agent as it is added to the control volume, $\dot q_{i,gas}$ is the radiant energy absorbed or loss by the gas, and $\dot q_{i,w,c}$ is the convective heat loss to a surface.

2.4.2 Buoyancy Head

The ($\rho g \Delta Z$) represents the buoyancy head through a junction or in a duct. It represents the head or force that results from any density gradient between the two endpoints of the junction or duct. For a junction the buoyancy head is given by:

$$(\rho g \Delta Z)_j = \left((\rho_k - \rho_i)\left(z_j + \frac{1}{2}\Delta z_j \right) + \rho_i \left(z_i + \frac{1}{2}\Delta z_i \right) - \rho_k \left(z_k + \frac{1}{2}\Delta z_k \right) \right) g \tag{16}$$

For a duct the buoyancy head is given by:

$$(\rho g \Delta Z)_d = \rho_d (z_{n2} - z_{n1}) g \tag{17}$$

If either node n1 or n2 is a terminal, then the compartment density gradient term, $\rho_i \left(z_i + \frac{1}{2}\Delta z_i \right)$, must be included in the manner of Equation 16.

2.4.3 Loss Terms

Pressure losses occur in junctions and in ducts and duct nodes. Junction pressure losses are estimated as a discharge coefficient whose value is a function of the type of opening. These losses are represented by the K in the momentum equation. It is assumed that direction through a junction does not impact the flow loss. Thus, only one K is needed. Ducts are more complex as they tend to contain fittings whose loss is direction dependent such as an expansion joint or a tee. Ducts also have a wetted length that tends to be much larger than the depth of a typical door like opening. Thus, there is the need to compute a wall friction loss. The basic equation for determining the net pressure loss in a duct is given by (Crane, 1988):

$$\Delta P_{loss,d} = \frac{\rho_d}{2} \sum_s \left(\frac{4 f L_s}{d_s} + \sum_i K_{i,s} \right) v_s^2 \tag{18}$$

where f is a wall friction factor, s is a duct segment of constant diameter, and i is a fitting. The friction factor is determined by the duct segment's Reynolds number and wall roughness, ε, as determined by the Colebrook Equation. As this equation requires an iterative solution, a direct solution approximation is used (George, et al., 2000a):

$$\frac{1}{\sqrt{f}} = -2\log\left(\frac{\varepsilon/d}{3.7} - \frac{4.518}{Re_d} \log\left(\frac{6.9}{Re_d} + \left(\frac{\varepsilon/d}{3.7} \right)^{1.11} \right) \right) \tag{19}$$

In FSSIM, ducts have unidirectional flow. Thus, as long as a length of duct is not interrupted by either terminating in a compartment or in a fitting with multiple other ducts (e.g.

where more than one exit flow path exists), this can be considered one duct for the purpose of the hydraulic calculation. However, this means that one duct could have multiple cross sectional areas. To avoid having to store the duct segment information, an effective loss can be determined. The loss is a function of velocity, and in the case of the wall friction, the diameter as well. Since a duct has unidirectional flow and no mass storage, the volumetric flow rate through any cross section of a duct is constant. Thus, all losses can be expressed in terms of a single diameter. The following derivation is shown to demonstrate how this is accomplished. FSSIM does not perform this calculation internally, but rather the user would need to do this when defining the duct for input.

$$K_s v_s^2 = K_{eq} v_{eq}^2, \quad v_{eq}^2 A_{eq} = v_s^2 A_s, \quad K_{eq} = K_s \frac{v_s^2}{v_{eq}^2} = K_s \frac{A_{eq}}{A_s} \tag{20}$$

$$\frac{f_s L_s}{d_s} v_s^2 = \frac{f_{eq} L_s}{d_{eq}} v_{eq}^2, \quad f_{eq} = \frac{f_s d_{eq}}{d_s} \frac{v_s^2}{v_{eq}^2} = \frac{f_s d_{eq}}{d_s} \frac{A_{eq}}{A_s} \tag{21}$$

The friction factors would still require computation at each time step, as they are dependent on a complex relationship with the Reynolds number. However, if fully turbulent flow is assumed in the duct, then f depends only on the wall roughness and duct diameter. With this assumption:

$$\Delta P_{loss,d} = \frac{\rho_d}{2} K_d v_d^2, \quad K_d = \sum_s \left(\frac{4 f L_s}{d_s} + \sum_i K_{i,s} \right) \frac{A_{eq}}{A_s} \tag{22}$$

In addition to losses along a contiguous length of duct, there are losses associated with the joining of multiple duct lengths such as a tee or manifold. If there are n ducts connected to node, then there will be n(n-1) possible combinations of inlet and outlet flow. For each incoming flow direction there is a loss associated with that incoming flow exiting the other flow directions given n(n-1) form losses. Computing the added loss in a ductnode is done before each iteration based on the prior iteration's velocity and density solution. First, each inlet duct is assigned a weighting factor based on its incoming flow fraction. Each outlet duct is then assigned a loss based on the weighted sums of the incoming flow loss times the appropriate form loss factor. The calculated equivalent loss, K_d, is used for K_j in Equation 9.

2.4.4 Bidirectional Flow

Two submodels for bidirectional flow are used in FSSIM. The first model is for horizontal flow through vertical openings (e.g. doors). The second model is for vertical flow through horizontal openings (e.g. hatches). The horizontal flow model uses the neutral plane concept and the assumption of linear pressure gradients within compartments (Karlsson and Quintiere, 2000) to determine at the beginning of each time step how a junction is to be partitioned. The vertical flow model is based on the work performed by Cooper (1989).

2.4.4.1 Bidirectional Horizontal Flow Submodel

Horizontal flow in an opening between compartments is driven by differences in relative pressure over the height of the opening. If each compartment's pressure is known at its floor and each compartment is at a uniform density, then the pressure as a function of height for each compartment can be given as:

$$P_i(z) = P_i(z_0) - \rho_i g(z - z_0) \tag{23}$$

The differential pressure in the opening is given as:

$$\Delta P_j(z) = P_i(z_{i,0}) - P_k(z_{k,0}) + \rho_k g(z - z_{k,0}) - \rho_i g(z - z_{i,0}) \tag{24}$$

If the differential pressure is positive, then flow will be from compartment i to k at that elevation, and the flow will be in the reverse direction if the differential pressure is negative. If the sign of the differential pressure changes over the height of an opening, then there will be bidirectional flow. The location of the neutral plane, the location where the pressure differential is zero, is given by:

$$z = \frac{P_k(z_{k,0}) - P_i(z_{i,0}) + g(\rho_k z_{k,0} - \rho_i z_{i,0})}{g(\rho_k - \rho_i)} \tag{25}$$

Each horizontal flow junction is represented by the model as two parallel junctions. By applying Equation 25 at the beginning of each time step the flow acceleration through the junction can be partitioned for bidirectional flow. To preserve the prior time step mass flow through the junction the velocities at the beginning of a times tep need to be adjusted by the computed change in flow area. To avoid numerical stability problems, the junction area change is relaxed and neither parallel junction is allowed to be less than 10 % of the flow area.

2.4.4.2 Bidirectional Vertical Flow Submodel

A strict application of Equation 4 would result in all horizontal openings having unidirectional flow. Since each compartment is represented by one set of quantities and the opening has no elevation change, as it is horizontal, the pressure change across the opening is uniform. In reality, however, unstable flow conditions may exist at these openings if cold dense air is above warmer less dense air. If denser gas is located in the upper compartment, depending upon the vent conditions there may be flow in both directions. Bidirectional flow will occur through a horizontal opening unless the pressure difference exceeds a flooding criterion. This criteria, where C_s is a shape factor equal to 0.754 for a circular opening, is (Cooper, 1989):

$$\left|\Delta P_{j,flood}\right| = \frac{C_s^2 g|\rho_i - \rho_k| D^5}{2F_j^2 A_j^2} = \frac{0.754^2 g|\rho_i - \rho_k| \sqrt{F_j A_j} \left(\frac{4}{\pi}\right)^{2.5}}{2} \tag{26}$$

Cooper's correlations for vertical flow involve a three-step process. First, the flowrate is determined as normal (e.g. assuming unidirectional flow). Second, the flooding limit is determined. Third, if the flooding limit has not been exceeded an exchange flowrate is calculated along with a new flowrate in the opposite direction such that the sum of the flowrates is equal to the first step. The exchange flowrate is given as:

$$v_{j,ex} = v_{j,ex\,max}\left(1 - \frac{|\Delta P_j|}{|\Delta P_{j,flood}|}\right);\ v_{j,ex\,max} = 0.055\frac{4A_j}{\pi}\sqrt{\frac{8g\Delta g_j F_j A_j}{\pi(\rho_i + \rho_k)}} \tag{27}$$

The $v_{j,ex}$ in the above equation represents a steady-state velocity. Equation 4 states that steady state will be reached when the pressure across an opening equals the loss through the opening. Thus, Equations 4 and 27 can be combined to yield a finite differenced, time derivative form of the exchange flow:

$$\begin{aligned} &v_{j,ex}^n + \frac{K_j}{2L_j}\left|v_{j,ex}^{n-} - v_{j,ex}^{n+}\right|v_{j,ex}^n = v_{j,ex}^{n-1} + \\ &\sigma_{j,ex}\frac{\Delta t^n}{L_j}\frac{1}{2}K_j\left(0.055\frac{4F_j^n A_j}{\pi}\sqrt{\frac{8g\Delta g_j F_j^n A_j}{\pi(\rho_i + \rho_k)}}\left(1 - \frac{|\Delta P_j|}{|\Delta P_{j,flood}|}\right)\right)^2 + \frac{K_j\Delta t^n}{2L_j}\left|v_{j,ex}^{n+}\right|v_{j,ex}^{n-} \end{aligned} \tag{28}$$

The $\sigma_{j,ex}$ is a direction function that will allow for flow acceleration along the proper direction for the exchange flow. For flow in the primary direction the v_j terms in Equation 14 are replaced by $v_j + v_{j,ex}$.

2.4.5 Specific Heat

The equation of state used is the ideal gas law expressed in energy, Equation 6. This equation relates the enthalpy of the gases in a compartment to the compartment temperature by means of the specific heat:

$$E_i^n = M_i^n T_i^n c_p\left(T_i^n\right) \tag{29}$$

The specific heat is a non-linear function of temperature. Thus, determining the value of the specific heat required for a particular compartment enthalpy, which is a conserved quantity, and pressure state requires simultaneously determining the compartment temperature. This can be done in an iterative fashion. A guess at the compartment temperature is made using the prior value for c_p and the current enthalpy. This temperature is used to re-evaluate c_p using the Newton-Raphson method (Hildebrand, 1976), and the process is repeated until c_p and temperature converge. This same process can be used for determining the effective temperature of a duct node given its pressure and incoming flows.

2.5 Combustion

2.5.1 Ignition

As part of the FSSIM input, users can define one or more fires to start at explicit times. User's may also choose to allow fire to spread. Ignition of additional fires is determined at the beginning of each time step. Each compartment can have a usetype designated for it, which denotes a fuel loading and fuel classification. Separate temperature ignition criteria can be defined for surfaces, temperature of incoming vent flows, and compartment temperature (Back, et al., 2003). Overhead surfaces can be given a different ignition temperature from non-overhead surfaces.

2.5.2 Pyrolysis

Pyrolysis is determined by one of three methods: the fire has a constant pyrolysis rate, a t^2 pyrolysis rate, or a user-defined pyrolysis rate. Growth in pyrolysis can be limited by specifying a maximum pyrolysis rate in kg/m^2-s. All fires can be given an end time in either absolute time or fuel loading. The calculated pyrolysis rate can be reduced be various mechanisms. If the fire is being suppressed by an agent, the pyrolysis will be reduced by a suppression factor. If the fire has become oxygen limited, then the pyrolysis rate is determined by a linear function of temperature. The maximum pyrolysis rate after oxygen-limiting conditions are reached is set at the point where the fire became oxygen limited; the compartment temperature for that point is also stored. The oxygen-limited pyrolysis rate is then calculated by the ratio of the current temperature to the stored temperature not to exceed the maximum rate.

2.5.3 Combustion Heat Release + Species Production

Combustion of pyrolyzed fuel is calculated on the basis of the available oxygen in the compartment where the pyrolysis is occurring. Currently, there is no burning of unburnt fuel exiting one oxygen-depleted compartment into a second oxygen-rich compartment. If there is sufficient oxygen in the compartment above a user specified lower limit, all the pyrolyzed fuel will combust. If there is insufficient oxygen in the compartment, a more detailed estimate of the available oxygen is made which includes a prediction of the net inflow of oxygen based on prior time step velocities. The actual heat release rate is adjusted to use the calculated amount of available oxygen. Note that a fire in an oxygen depleted compartment can burn at a rate equal to the pyrolysis if there is a sufficient flowrate of oxygen into the compartment.

Species are generated based on user-provided yields for each fuel being burned. These yields represent the mass of combustion products formed for a unit mass of fuel burned. Note that the consumption of oxygen can be expressed as a negative yield.

2.6 Overall Solution Scheme

An iterative solution scheme is used to solve the hydraulic equations. This scheme consists of time step initialization, an outer loop, an inner loop, and a time step wrap-up. The outer loop goal is convergence of the compartment pressure solution and prevention of large changes in thermophysical conditions over a time step. The inner loop goal is convergence of the junction

and duct velocity solution along with conservation of mass at duct nodes. The flow chart in Figure 2 shows the iteration logic.

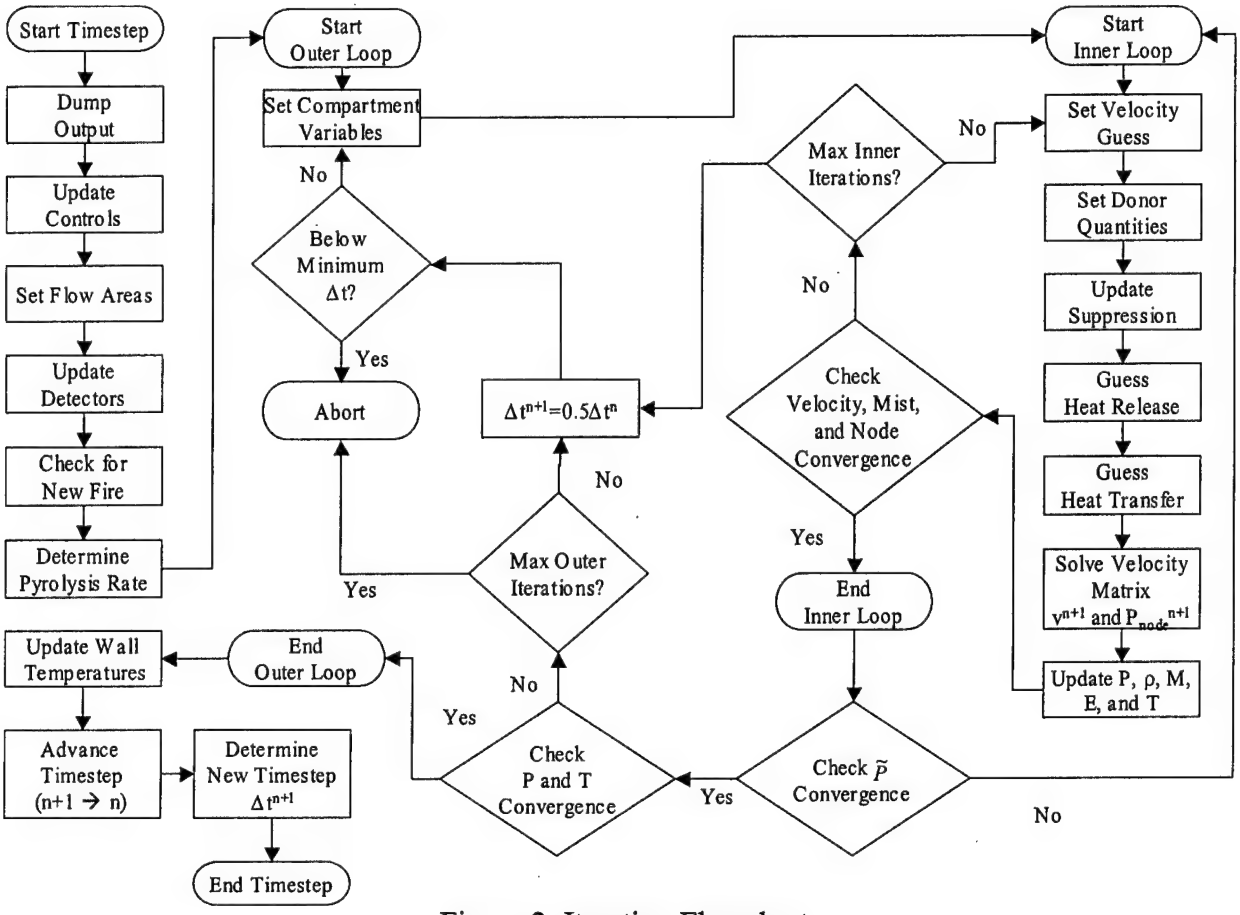

Figure 2: Iteration Flowchart

2.6.1 Time step Initialization

Before entering the outer loop, the time step initial conditions are established. Output is dumped if a user-defined output interval has elapsed. All control functions are evaluated using a recursive routine; the recursion allows for control functions that are functions of other control functions. The available flow area of junctions and ducts are determined. Finally, compartments are checked for ignition of a new fire, and any existing fire's pyrolysis rate is determined.

2.6.2 Outer Loop

A time step starts outside the outer loop. End of time step c_p values for each compartment are predicted from the prior time step solution. The inner loop is then executed. Upon exiting the inner loop, the $\tilde{P}_i$ values used in Equation 14 are compared to solution values, P_i^n. If the difference in value is below a convergence criteria, the time step is advanced. This step ensures that linearized pressure relations for mass flows used in the momentum equation were reasonable at the end of the time step. If not, the outer loop is cycled and the $\tilde{P}_i$ values will be

approximated using the prior iteration's solution. If the $\tilde{P}_i$ values are converged, then the velocities, temperatures, and pressures are checked for their relative change and a Courant criterion is checked. If any of the associated limits, to be discussed later, are exceeded the time step is reduced and the outer loop is cycled. Lastly, the new time step size is determined by determining the variable that was closest to exceeding its convergence criteria. The new time step is given a multiplier and the current time step. The multiplier is the ratio of the closest convergence to its associated criteria not to exceed a user-defined maximum time step. If either too many outer loops iterations or too small of a time step occurs, then the time step will fail and the calculation will abort.

2.6.3 Inner Loop

The inner loop constructs and solves the matrix for the duct and junction momentum equations and mass conservation at internal duct nodes. However, since the new velocities are a function of the energy source terms in each compartment, the inner loop also updates the source terms for each iteration. The first step in the inner loop is setting the v^{n+} values by examining ducts and junctions for flow reversal. Second, donor values are determined using Equation 5. The prior iteration velocities and source terms are used to generate the $c_{p_i}^{n+}$ values in Equation 13. The compartment heat release rate is then determined along with the effects of suppression systems. Convective and radiative heat transfer are then determined for each compartment. The solution matrix is constructed, zero-value columns and rows are eliminated (resulting from ducts and junctions that have dampers or doors closed), and the matrix solved. Equations 7 and 8 are used to update compartments and duct nodes. The velocities and duct node mass conservation are checked for convergence, criteria to be discussed later. If the criteria are not met, the inner loop is cycled. If the number of inner iterations exceeds a user specified criteria, the inner loop is exited, the time step reduced, and the outer loop is cycled.

If the inner loop is cycled a partial update is performed of the energy source terms. Heat release rates are updated in ventilation-controlled compartments using the new velocity solution; this is not needed in non-ventilation controlled compartments as their heat release rate is not a function of incoming mass flows. The radiation solution is updated in compartments containing a fire using the newly predicted compartment and surface temperatures resulting from the current velocity solution. Non-burning compartments are not updated in order to reduce computational time; their radiation source term is not likely to vary significantly from the first iteration. Lastly, surface heat fluxes are recomputed.

2.6.4 Time step Wrap-up

After successful completion of the outer loop, the time step is advanced. A final update is performed on the surface temperatures. All other variables are also updated by setting all prior time step values to the newly calculated values. Lastly, the simulation clock is advanced.

2.6.5 Convergence Criteria

2.6.5.1 Inner Convergence Criteria

There are three sets of convergence criteria for the inner iterations. The first criterion is for the mass conservation for a duct node. The second set is for the velocity in ducts. The third set of criteria is for velocity in junctions. Mass conservation is determined by calculating the net mass flow at a duct node and the sum of the absolute value of the mass flows at a duct node. If conservation is met, the net mass flow should be zero; however, round off error in the floating point math may prevent this. Instead, the net mass flow is compared to the total mass flow, and if the error is greater than 0.001 %, the inner loop is cycled. The duct and junction velocity criteria have similar logic but can be set with different values for convergence. For each duct and junction, if the flow area was nonzero, and the velocity magnitude of the prior time step and current solution are both above a cutoff, currently 1 μm/s, convergence is checked. Without the cutoff junctions and ducts with essentially zero flow that have no impact on the overall mass exchange could prevent convergence. Two criteria are then checked. The first is flow reversal; if the flow in a duct or junction changes direction, the inner iteration is repeated. The second is the relative change in velocity. If the relative change in velocity between iterations is greater than 5%, the inner iteration is cycled.

2.6.5.2 Outer Convergence Criteria

There are two sets of convergence criteria for the outer loop. The first compares the $\tilde{P}_i$ values used in Equation 14 to the solution values, P_i^n. If they differ by more than 1 %, the outer iteration is repeated without a change in time step. This criterion ensures that the thermophysical properties assumed during the solution reflect the end of time step values for those properties. The second set of criteria examines the relative change in temperature, mass flows, and pressures. Specifically, if temperature in any compartment changes by more than 10 %, pressure in any compartment changes by more than 1 %, or the net mass flow for a compartment exceeds 50 % of the end of beginning of time step mass, then the outer loop is cycled with a reduced time step. The time step reduction is the larger of 50 % or the largest percentage by which any convergence criterion was exceeded.

3.0 HEAT TRANSFER SOLVERS

3.1 Convection

Convection heat transfer is calculated for each surface for each time step using the beginning of time step surface and compartment temperatures. Depending on the surface orientation, horizontal or vertical, one of two natural convection heat transfer correlations are used to determine the convective heat transfer. The correlations used are (Holman, 1990):

Horizontal: heated facing downward or cooled facing upward

$$\dot{q}''^{,n}_{i,w} = 0.59\left|\frac{T_i^n - T_w^n}{L}\right|^{1/4}\left(T_i^n - T_w^n\right) \tag{30}$$

Horizontal: heated facing upward or cooled facing downward

$$\dot{q}''^{,n}_{i,w} = 1.52\left|T_i^n - T_w^n\right|^{1/3}\left(T_i^n - T_w^n\right) \tag{31}$$

Vertical

$$\dot{q}''^{,n}_{i,w} = 1.24\left|T_i^n - T_w^n\right|^{1/3}\left(T_i^n - T_w^n\right), \tag{32}$$

where i indicates a compartment, L is a characteristic length of the surface (taken as the square root of the surface area), and w indicates a surface.

3.2 Radiation

Radiation heat transfer is computed on a compartment-by-compartment basis using the beginning of time step surface temperatures, compartment temperature, compartment gas composition, and compartment heat release rate. The heat transfer is calculated using a modified gray-gas, n-surface net radiation method (Forney, 1991).

3.2.1 Net Radiation Equation Derivation

The radiation heat transfer equation for a surface is:

$$A_w \sigma \varepsilon_w T_w^4 + (1-\varepsilon_w)\dot{q}''^{in}_w = \dot{q}^{in}_w + A_w \Delta\dot{q}''_w \tag{33}$$

with

$$A_w \Delta\dot{q}''_w = \dot{q}^{out}_w - \dot{q}^{in}_w \tag{34}$$

$$\dot{q}_w^{out} = A_w \sigma \varepsilon_w T_w^4 + (1-\varepsilon_w)\dot{q}_k^{in} \tag{35}$$

$$\dot{q}_w^{in} = \sum_{w2} \dot{q}_{w2}^{out} F_{w2-w} \tau_{w2-w} + c_w, \tag{36}$$

where $F_{w2\text{-}w}$ is the view factor from surface w2 to w. In the absence of attenuation or scatter this is the fraction of energy leaving w2 that arrives at w. τ is the transmission factor from surface w2 to w, the fraction of energy transmitted over the distance between surface w2 and w. c_w is a source term representing such as radiant emissions from a fire or hot gasses in the compartment. Δq represents the net radiant heat transfer, and ε is the surface emissivity.

If Equations 33 through 36 are combined in conjunction with the view factor symmetry relationship, $A_w F_{w\text{-}w2} = A_{w2} F_{w2\text{-}w}$, an equation for the net heat transfer can be derived.

$$\frac{\Delta \dot{q}_w''}{\varepsilon_w} - \sum_{w2} \frac{1-\varepsilon_{w2}}{\varepsilon_{w2}} \Delta \dot{q}_{w2}'' F_{w2-w} \tau_{w2-w} = \sigma T_w^4 - \sum_{w2} \sigma T_{w2}^4 F_{w-w2} \tau_{w-w2} - \frac{c_w}{A_w} \tag{37}$$

Since it is numerically possible for the emissivity of a surface to be zero, the above equation is modified by the substitution

$$\Delta \tilde{q}_w'' = \varepsilon_w \Delta \dot{q}_w'' \tag{38}$$

$$\Delta \tilde{q}_w'' - \sum_{w2} (1-\varepsilon_{w2}) \Delta \tilde{q}_{w2}'' F_{w2-w} \tau_{w2-w} = \sigma T_w^4 - \sum_{w2} \sigma T_{w2}^4 F_{w-w2} \tau_{w-w2} - \frac{c_w}{A_w} \tag{39}$$

This results in a dense matrix, the only zero terms are for surfaces along the same wall, which can be solved by using a number of numerical techniques. This matrix will, however, always be diagonally dominant since $0 \le \varepsilon \le 1$. The transmission factor is calculated by assuming a gray gas and it is given by

$$\tau_{w2-w} = e^{-\alpha L_{w2-w}}, \tag{40}$$

where α is an absorption coefficient which is calculated based on the amounts of CO_2, H_2O, and soot in the compartment along with an average pathlength. L represents an average path length between two radiatively communicating surfaces. Note that this is not the same pathlength used for calculating α. α is calculated using the ABSORB subroutine from CFAST v3.1.7 (Jones, et al., 2000). This routine calculates α by doing a table lookup of absorptivities of the CO_2 and H_2O mass fractions and accounting for band overlap, which can be approximated as one half of the CO_2 absorptivity (Tien, Lee, and Stretton, 2002). The net α is calculated by summing the table values with a contribution due to soot:

$$\alpha_{gas} = \alpha_{H_2O} + \alpha_{CO_2} - \frac{1}{2}\alpha_{CO_2} \tag{41}$$

$$\alpha_{net} = 1.4 k_s V_{i,s} T_i - \frac{\ln(1 - \alpha_{gas})}{L_i}, \tag{42}$$

where k_s is an empirical constant (k_s=1195), $V_{i,s}$ is the soot volume fraction in compartment i, T_i is the gas temperature, and L_i is the beam length calculated with Equation 44.

The source term, c_w, is determined by assuming a gray gas and that the fire radiates a fixed fraction of its heat release as radiant energy.

$$c_w = F_{f-w}\tau_{f-w}\chi_f \dot{q}_f + \sum_{w2}(1-\tau_{w2-w})F_{w-w2}\sigma T_i^4, \tag{43}$$

where χ is the radiant fraction of the fire.

3.2.2 Solution of the Net Radiation Equation

To simplify the solution of equation 39 three assumptions are made. First, each compartment is assumed to be a rectangular parallelepiped. Every surface in each compartment is then associated with one of the six surfaces of the parallelepiped. Second, the view factor of any subsurface for a wall of the parallelepiped is determined from the area fraction of that surface with respect to the parallelepiped wall containing it. Third, the fire is located at the center of the parallelepiped and "paints" the walls based on their area fraction with respect to the total compartment surface area. The calculation of pathlengths and view factors is greatly simplified by these assumptions.

Pathlengths for fire radiation to the surfaces is calculated as one half of the compartment dimensions. Thus, the pathlength from the fire to the floor or ceiling is given as one half the height of the compartment. Pathlengths for surface-to-surface communication is calculated as the parallelepiped wall center-to-wall center distance. Thus, the floor-to-ceiling pathlength is the height of the compartment and the ceiling-to-sidewall pathlength would be the diagonal line connecting the ceiling center to the side center. For the purpose of calculating absorption coefficients the pathlength is calculated as shown below (Holman, 1990):

$$L_i = \frac{3.6 V_i}{\sum_w A_w} \tag{44}$$

View factors from the fire to the surfaces are calculated solely on the basis of the area fraction of the wall with respect to the entire compartment.

$$F_{f-w} = \frac{A_w}{\sum_w A_w} \tag{45}$$

Surface view factors are calculated as either parallel-plate view factors or right-angle-corner view factors based on the parallelepiped walls to which the surfaces belong to. The view factor

of each surface is given as the appropriate wall view factor times the area fraction of the surface with respect to that wall. Parallel-plate view factors are given as:

$$F = \frac{2}{\pi xy}\left(\begin{array}{l} \ln\left(\frac{(1+x^2)(1+y^2)}{1+x^2+y^2}\right) + x\sqrt{1+y^2}\tan^{-1}\left(\frac{x}{\sqrt{1+y^2}}\right) + \\ y\sqrt{1+x^2}\tan^{-1}\left(\frac{y}{\sqrt{1+x^2}}\right) - x\tan^{-1}x - y\tan^{-1}y \end{array}\right), \tag{46}$$

where x and y are the ratios of each side to the plate separation. Corner view factors are given as:

$$F_{1\text{-}2} = \frac{1}{\pi X}\left(\begin{array}{l} X\tan^{-1}\frac{1}{X} + Y\tan^{-1}\frac{1}{Y} - \sqrt{X^2+Y^2}\tan^{-1}\sqrt{\frac{1}{X^2+Y^2}} + \\ \frac{1}{4}\ln\left(\frac{(1+X^2)(1+Y^2)}{1+X^2+Y^2}\left(\frac{X^2(1+X^2+Y^2)}{(1+X^2)(X^2+Y^2)}\right)^{X^2}\left(\frac{Y^2(1+X^2+Y^2)}{(1+Y^2)(X^2+Y^2)}\right)^{Y^2}\right) \end{array}\right), \tag{47}$$

where z is the length of the common side, x and y are the lengths of the other two sides of rectangles 1 and 2, respectively, X= x/z, and Y=y/z (Siegel, et al., 2001)

The first part of the solution is to construct the right hand side vector for the net radiation matrix. This vector consists of the source term representing radiative inputs from the fire and the gas as well as the direct emissions from the surfaces; reflected emissions are part of the net radiation terms on the left-hand side.

$$\begin{array}{l} \sigma T_w^4 - \sum_{w2}\sigma T_{w2}^4 F_{w-w2}\tau_{w-w2} - \frac{c_w}{A_w} = F_{f-w} = \\ \sigma T_w^4 - \sum_{w2}\sigma F_{side(w)\text{-}side(w2)}\frac{A_{w2}}{A_{side(w2)}}e^{-L_{side(w)\text{-}side(w2)}\alpha_i}T_{w2}^4 - \frac{A_w\chi_f\dot{q}_f}{\sum_w A_w}e^{-L_{f-side(w)}\alpha_i}, \\ -\sigma T_i^4\sum_{w2}F_{side(w)-side(w2)}\left(1-e^{-L_{side(w)-side(w2)}\alpha_i}\right) \end{array} \tag{48}$$

where side(w) indicates the compartment face that contains surface w.

The left-hand side is constructed as follows:

$$\underline{A}\,\Delta\vec{\tilde{q}}_w'' = \left|\begin{array}{l} A_{w,w2:w=w2} = 1 \\ A_{w,w2:w\neq w2} = -\frac{A_w}{A_{side(w)}}F_{side(w)-side(w2)}e^{-L_{side(w)-side(w2)}\alpha_i}\left(1-\varepsilon_{w2}\right) \end{array}\right|\Delta\vec{\tilde{q}}_w'' \tag{49}$$

After solving the matrix the net radiation is extracted from the modified net radiation. In both Equations 48 and 49 the treatment of the gas and surface temperatures depends on the current inner iteration. For the first iteration, they are taken from the previous time step's solution. For subsequent inner iterations, they are taken as the average of the previous time step and the previous iteration. At high temperatures, small changes value can have large changes in the radiative field. By taking the average of the prior time step and the prior iteration, this effect can be minimized.

$$\Delta q_w = \Delta \tilde{q}''_w \varepsilon_w A_w \tag{50}$$

The net radiation absorption by the gas is determined by the difference in the total net radiation to the surfaces and the radiative output of the fire. Any difference between these two values results from a net emission or a net absorption by the gas in the compartment.

$$\Delta \dot{q}_i = \chi_f \dot{q}_f + \sum_w \Delta \tilde{q}''_w \varepsilon_w A_w \tag{51}$$

3.3 Conduction

3.3.1 1D Conduction Equation

Conduction heat transfer is computed for each surface at the end of each time step using the beginning of time step computed convective and radiative heat transfer solutions as boundary conditions. Heat conduction is calculated using a 1D solver with multiple layers of materials and temperature-dependent specific heats and conductivities. The general equation for 1D heat transfer in Cartesian coordinates is (Holman, 1990):

$$\frac{\partial}{\partial x} k \frac{\partial T}{\partial x} + \dot{q}''' = \rho c \frac{\partial T}{\partial t}, \tag{52}$$

where k is the conductivity, ρ is the material density, $\dot{q}'''$ is a volumetric heat generation rate, T is the material temperature, x is the position within the material, and c_p is the material specific heat. In general k, ρ, and c are all functions of temperature. However, allowing ρ to be a function of temperature means the solution would either have to take into account expansion of the material which adds greatly to the required computation resources required, or conservation of mass would not be maintained which is also undesirable. At the boundaries the following holds:

$$q''_w = -k \left. \frac{dT}{dx} \right|_w, \tag{53}$$

where w is the material surface and q''_w is the net surface heat flux.

3.3.2 Solution of 1D Conduction Equation

To solve Equation 52 a few simplifications are made: no internal heat generation, no removal of material from a surface (e.g. as would represent mass loss from pyrolysis), and constant density (though there is temperature-dependent conductivity and specific heat). The equation is discretized with central differences in space and with an implicit Crank-Nicholson scheme in time (Strauss, 1992). The 1D surface is divided into N-1 cells or nodes with N boundaries. Temperatures are stored at the boundary locations. Thermophysical properties are explicit from the previous time step solution. The general form of the spatial discretization is:

$$\frac{1}{2}\left(\Delta x_{i-\frac{1}{2}}\rho_{i-\frac{1}{2}}c_{i-\frac{1}{2}}+\Delta x_{i+\frac{1}{2}}\rho_{i+\frac{1}{2}}c_{i+\frac{1}{2}}\right)\frac{dT_i}{\Delta t^n}=k_{i-\frac{1}{2}}\left(\frac{T_{i-1}-T_i}{\Delta x_{i-\frac{1}{2}}}\right)+k_{i+\frac{1}{2}}\left(\frac{T_{i+1}-T_i}{\Delta x_{i+\frac{1}{2}}}\right), \tag{54}$$

where i is a node and Δx is a node spacing. Discretization of the time step yields:

$$T_i^n=T_i^{n-1}+\Delta t^n\frac{1}{\left(\Delta x_{i-\frac{1}{2}}\rho_{i-\frac{1}{2}}c_{i-\frac{1}{2}}+\Delta x_{i+\frac{1}{2}}\rho_{i+\frac{1}{2}}c_{i+\frac{1}{2}}\right)}\frac{1}{2}\left(\begin{array}{l}k_{i-\frac{1}{2}}\left(\frac{T_{i-1}^n-T_i^n}{\Delta x_{i-\frac{1}{2}}}\right)+k_{i+\frac{1}{2}}\left(\frac{T_{i+1}^n-T_i^n}{\Delta x_{i+\frac{1}{2}}}\right)+\\ k_{i-\frac{1}{2}}\left(\frac{T_{i-1}^{n-1}-T_i^{n-1}}{\Delta x_{i-\frac{1}{2}}}\right)+k_{i+\frac{1}{2}}\left(\frac{T_{i+1}^{n-1}-T_i^{n-1}}{\Delta x_{i+\frac{1}{2}}}\right)\end{array}\right) \tag{55}$$

$$\begin{aligned}T_i^n-\Delta t^n\frac{k_{i-\frac{1}{2}}\left(\frac{T_{i-1}^n-T_i^n}{\Delta x_{i-\frac{1}{2}}}\right)+k_{i+\frac{1}{2}}\left(\frac{T_{i+1}^n-T_i^n}{\Delta x_{i+\frac{1}{2}}}\right)}{2\left(\Delta x_{i-\frac{1}{2}}\rho_{i-\frac{1}{2}}c_{i-\frac{1}{2}}+\Delta x_{i+\frac{1}{2}}\rho_{i+\frac{1}{2}}c_{i+\frac{1}{2}}\right)}=\\ T_i^{n-1}+\Delta t^n\frac{k_{i-\frac{1}{2}}\left(\frac{T_{i-1}^{n-1}-T_i^{n-1}}{\Delta x_{i-\frac{1}{2}}}\right)+k_{i+\frac{1}{2}}\left(\frac{T_{i+1}^{n-1}-T_i^{n-1}}{\Delta x_{i+\frac{1}{2}}}\right)}{2\left(\Delta x_{i-\frac{1}{2}}\rho_{i-\frac{1}{2}}c_{i-\frac{1}{2}}+\Delta x_{i+\frac{1}{2}}\rho_{i+\frac{1}{2}}c_{i+\frac{1}{2}}\right)}\end{aligned} \tag{56}$$

Boundary conditions are implemented by assuming one of two boundary conditions. The first time through the solver the boundary condition is a constant radiative heat flux and a constant convective heat transfer coefficient based on the beginning of time step compartment temperature and radiative conditions from Equations 30 - 32 and 50. The radiative flux is

corrected for the new surface temperature to avoid instabilities at high surface temperatures. This correction is performed by linearizing the radiative heat transfer change as follows:

$$\frac{d\dot{q}_w^{out}}{dT_w} = 4\varepsilon_w \left(T_w^{n-1}\right)^3 \left(T_w^n - T_w^{n-1}\right) \tag{57}$$

If the time step decreases during an iteration, the heat transfer solution is repeated with a constant heat flux condition equal to the sum of the constant radiative flux and the time-average convective flux determined from the first pass through the solver. At the i=1 and i=N surfaces, the general discretized equation for the first pass through the solver becomes:

$$T_1^n - \frac{\Delta t^n}{\Delta x_{\frac{3}{2}} \rho_{\frac{3}{2}} c_{p,\frac{3}{2}}} \left(\frac{k_{\frac{3}{2}}}{2} \frac{T_2^n - T_1^n}{\Delta x_{\frac{3}{2}}} \right) + \frac{\Delta t^n}{\Delta x_{\frac{3}{2}} \rho_{\frac{3}{2}} c_{p,\frac{3}{2}}} \left(\frac{h_1}{2} \left(T_1^n\right) + 4\varepsilon_1 \left(T_1^{n-1}\right)^3 T_1^n \right) =$$
$$T_1^{n-1} + \frac{\Delta t^n}{\Delta x_{\frac{3}{2}} \rho_{\frac{3}{2}} c_{p,\frac{3}{2}}} \left(\frac{h_1}{2} \left(2T_g^{n-1} - T_1^{n-1}\right) + q''^{n-1}_{1,rad} + 4\varepsilon_1 \left(T_1^{n-1}\right)^4 + \frac{k_{\frac{3}{2}}}{2} \frac{T_2^{n-1} - T_1^{n-1}}{\Delta x_{\frac{3}{2}}} \right) \tag{58}$$

$$T_N^n - \frac{\Delta t^n}{\Delta x_{N-\frac{1}{2}} \rho_{N-\frac{1}{2}} c_{p,N-\frac{1}{2}}} \left(\frac{k_{N-\frac{1}{2}}}{2} \frac{T_{N-1}^n - T_N^n}{\Delta x_{N-\frac{1}{2}}} \right) + \frac{\Delta t^n}{\Delta x_{N-\frac{1}{2}} \rho_{N-\frac{1}{2}} c_{p,N-\frac{1}{2}}} \left(\frac{h_N}{2} \left(T_N^n\right) + 4\varepsilon_1 \left(T_N^{n-1}\right)^3 T_N^n \right) =$$
$$T_N^{n-1} + \frac{\Delta t^n}{\Delta x_{N-\frac{1}{2}} \rho_{N-\frac{1}{2}} c_{p,N-\frac{1}{2}}} \left(\frac{h_N}{2} \left(2T_g^{n-1} - T_N^{n-1}\right) + q''^{n-1}_{N,rad} + 4\varepsilon_1 \left(T_N^{n-1}\right)^4 + \frac{k_{N-\frac{1}{2}}}{2} \frac{T_{N-1}^{n-1} - T_N^{n-1}}{\Delta x_{N-\frac{1}{2}}} \right) \tag{59}$$

Equations 56, 58, and 59 result in a tridiagonal matrix. The matrix is solved for the current time step using a tridiagonal solver and the relative difference in the new solution compared to the previous solution is calculated. The node-spacing values are selected automatically. The terminal nodes for each layer of a surface are set such that their Biot number is at least 0.1 with the heat transfer coefficient assumed to be 100 W/m^2-K. Node sizes progressing into a layer are obtained by successive doubling of the outer node size (for example: 0.1 m, 0.2 m, 0.4 m, 0.2 m, 0.1 m). This technique minimizes the number of nodes while maintaining a reasonable accuracy in the time-dependent solution (George, et al., 2000b). If the temperature change in any one cell exceeds a specified tolerance, currently 0.1%, the solution time step is divided by an integer factor representing the factor by which the tolerance was exceeded. The matrix is now solved within a loop, with the thermophysical parameters calculated at the start of each sub-time step.

After updating a surface, a correction is made to the radiation heat transfer to the gas. The radiant heat transfer boundary conditions in Equations 58 and 59 account for the change in surface temperature over a time step.

If the Biot number calculation for a single-layer surface results in only one node for that surface, the above method is not used. Instead, a lumped parameter analysis is performed where:

$$T^n = T^{n-1} + \frac{\Delta t^n}{\Delta x \rho c}\left(q_I''^{n-1} + q_N''^{n-1}\right) \tag{60}$$

4.0 MISCELLANEOUS

4.1 Control Functions

FSSIM has a limited capability to model control systems. Two types of control functions are available. The first type is a binary (on/off) control function which will change state from true to false, or vice versa, when a user-specified criterion, such as time or a compartment temperature, is reached. This function can be defined as a trip function. As a trip, the variable will only change state once, so if, for example, a temperature criterion is reached, the function will not change state if the temperature decreases below the setpoint. The second type of function is an AND gate which will change the state of a binary function when two specified conditions are true. This function type can be used to specify equipment operation based on some physical criteria along with an equipment state variable to indicate its ability to function.

4.2 Fire Detection Models

A number of detection devices are modeled by FSSIM. All of the detection devices, with the exception of UV or IR detectors, can be located in either a compartment or a duct.

4.2.1 Ionization/Photoelectric Detector

Ionization and photoelectric detectors will alarm based on a user provided optical depth; the default is 0.0581 m^{-1}. The optical depth is calculated as (Mulholland and Croarkin, 2000):

$$OD = \sigma_s \rho_s, \tag{61}$$

where ρ_s is the soot density and σ_s is the mass extinction coefficient of soot, 8700 m^2/kg.

4.2.2 Gas Detector

A gas detector will alarm when the gas it measures reaches a user-defined mass fraction.

4.2.3 Fixed Temperature Detector

A fixed temperature detector will alarm when the temperature it measures reaches a user-defined threshold.

4.2.4 RTI Detector

The RTI detector type simulates the response of a thermal activation link as might be present on a sprinkler head. The temperature change in the detector is given by:

$$T^n = \Delta t^n \left(\sqrt{v_{f\,or\,j}} \frac{T_{i\,or\,j} - T^{n-1}}{RTI} \right), \tag{62}$$

where $T_{i\,or\,j}$ is the temperature of the compartment or duct in which the detector is located and $v_{f\,or\,j}$ is either a ceiling jet velocity based on the compartment fire size or the duct velocity. In a compartment without a fire v_f=0.1 m/s and with a fire the velocity is calculated as:

$$v_f = \begin{cases} 0.95 \left(\dfrac{\dot{q}_f}{\Delta z_i} \right)^{1/3}, \dfrac{L_i}{\Delta z_i} \le 0.15 \\ \dfrac{0.2 \dot{q}_r^{1/3} \sqrt{\Delta z_i}}{L_i^{5/6}}, \dfrac{L_i}{\Delta z_i} > 0.15 \end{cases}, \tag{63}$$

where Δz_i is the height of the compartment and L_i is either one half the diagonal distance from the center of the upper surface to its corner, or one half a user-specified separation distance.

4.2.5 UV/IR Detector

The current model for a UV or IR detector serves as a placeholder. In its current implementation the detector will alarm when the fire reaches a user defined size.

4.3 Fire Suppression Models

4.3.1 Mist

Mist systems are assumed to extinguish a fire via displacement of oxygen due to evaporation. The mist model tracks both a mist droplet quantity and an evaporation quantity for the compartment in which the mist system is located. Currently, evaporation of mist from remote compartments, convective heating of droplets, droplet-droplet interactions, and droplet-surface heat transfer are not evaluated. The mist model involves two primary computations. The first is the time rate of change of droplet concentration resulting from mist nozzle discharge and droplet fallout. The second is the rate of evaporation, which is determined by available energy for evaporation and the compartment's equilibrium vapor mass fraction.

The droplet concentration at the end of a time step is given by:

$$\frac{dM_{mist}}{dt} = \dot{M}_{nozzle} - \dot{M}_{fallout} - \dot{M}_{evaporation} - \dot{M}_{outflow} \tag{64}$$

Fallout results from mist droplets impacting one of the surfaces of the compartment. If the droplets are traveling at their terminal velocity, the rate at which they fallout is given by the time it takes the droplets to travel from their location to a surface. Since the mist spray and compartment convection will distribute the mist widely throughout a compartment, there is no fixed droplet location; instead a mean beam length, Equation 44, is assumed. The terminal velocity and the mean beam length yield a time constant for the droplet fallout. Droplet terminal velocity is given by solving the equation below for the droplet terminal velocity, v_d:

$$M_d g = \frac{1}{2}\rho_i C_D \pi r_d^2 v_d^2, \tag{65}$$

where M_d is the droplet mass, C_D is the droplet drag coefficient, r_d is the droplet radius, and ρ_i is the compartment gas density. The drag coefficient is a function of the droplet Reynolds number and is given by (Clift, Grace, and Weber, 1978):

$$C_D = \begin{cases} \dfrac{24}{Re_d} & Re_d < 1 \\ \dfrac{24\left(1+0.15Re_d^{0.687}\right)}{Re} & 1 \le Re_d \le 1000 \\ 0.44 & 1000 < Re_d \end{cases} \tag{66}$$

Since the droplet Reynolds number, Re_d, is a function of the droplet velocity, the terminal velocity is determined by iteration. With terminal velocity known the droplet fallout rate is given by:

$$\dot{M}_{fallout} = -\frac{M_{mist}^{n-1}\left(1-e^{-\Delta t^n \frac{v_d}{L_i}}\right)}{\Delta t^n} \tag{67}$$

The evaporation of mist droplets is limited by four factors: the compartment equilibrium vapor mass fraction, the energy available for evaporation, the mass of available mist, and the convective/diffusive limitation on the droplet vaporization. The equilibrium vapor mass fraction can be given by the Clausius-Clapeyron equation (Wylen and Sonntag,1986) where X_v is the equilibrium mole fraction for water vapor:

$$X_V = e^{\frac{h_v mw_{H_2O}}{R}\left(\frac{1}{T_b}-\frac{1}{T_i}\right)} \tag{68}$$

where h_v is the heat of vaporization of water, mw_{H_2O} is the molecular weight of water, and T_b is the boiling temperature of water. Assuming the remaining gas is air, this is equivalent to a mass fraction of:

$$Y_V = \frac{X_V}{X_v\left(1-\frac{mw_{air}}{mw_{H_2O}}\right)+\frac{mw_{air}}{mw_{H_2O}}} \tag{69}$$

The energy available to evaporate the droplet is the sum of the droplet enthalpy and the convective heat transfer to the drop. The convective heat transfer is determined from the following correlation for heat transfer coefficient (Cheremisinoff, 1986):

$$h = \frac{\left(2+0.6Re_d^{1/2}Pr_{air}^{1/3}\right)k_{air}}{2r_d} \tag{70}$$

The rate at which the water can evaporate is limited by the diffusion and convection of water vapor away from the drops surface as it evaporates (Cheremisinoff, 1986):

$$\dot{M}_{evaporation} = n_d 2r_d \pi Sh_d \rho_{air} D_{H_2O} \ln\left(\frac{Y_{H_2O,i}-1}{Y_{H_2O,equil}-1}\right), \tag{71}$$

where D_{H_2O} is the diffusion coefficient of water vapor into air ($0.256x10^{-4}$ m^2/s), n_d is the number of droplets available for evaporation, and Sh_d is the droplet Sherwood number which is given by:

$$Sh_d = 2+0.6Re_d Sc_{air}, \tag{72}$$

where Sc is the Schmidt number.

The actual mist evaporation is calculated iteratively. Equations 70 and 71 are used along with the total available water mist, after accounting for any settling with Equation 67, to determine the maximum possible mist evaporation. A guess at the new end of time step compartment mass and energy content is made using the previous time step mass and energy and prior iteration change in mass and energy along with any change due to the predicted evaporation. From this a new compartment temperature can be determined. The equilibrium vapor mass fraction for this new temperature is compared with the guess of the new compartment vapor mass fraction. If the equilibrium is exceeded a bisection method is used to guess a mass of evaporation. This process is repeated at each inner iteration. In this manner the calculated evaporation should avoid any large violations of the equilibrium condition.

4.3.2 Sprinkler

The performance of a standard sprinkler system is evaluated using the method of Evans (1993). This method, resulting from analysis of experimental data, assumes that a fire is suppressed by a standard sprinkler system with a time constant, τ, given by:

$$\tau = 3\dot{w}''^{-1.85}, \tag{73}$$

where $\dot{w}''$ is the spray density in kg/m^2-s. Suppression is calculated as:

$$\dot{q}_{f,suppressed} = \dot{q}_f e^{\frac{t-t_{act}}{\tau}}, \quad (74)$$

where t_{act} is the activation time of the sprinkler system.

4.3.3 Gaseous

A gaseous suppression system will extinguish a fire once it displaces sufficient oxygen to bring the compartment oxygen mass fraction below a specified lower limit for combustion.

4.3.4 Hydroflourocarbon (HFC)

An HFC system will extinguish a fire once the agent reaches a specified extinguishment mass fraction.

4.3.5 Handline

No model implemented at this time.

4.3.6 Foam

The foam suppression model calculates a suppression factor which is equal to the fraction of the floor area that is covered by the foam. The area covered is calculated by using the foam flow rate, foam density, and foam layer thickness combined with the net time the foam system has been discharging. This model serves as a placeholder for future development of a more physically based model.

4.3.7 Dry Chemical

A dry chemical system will extinguish a fire once the agent reaches a specified extinguishment mass fraction.

4.3.8 Boundary Cooling

A functioning boundary cooling system is assumed to coat the entire surface being cooled with a film of water of constant temperature. The boundary cooling operates by replacing the heat transfer coefficient in Equations 30 through 32 with a constant heat transfer coefficient. This coefficient is either 3000 W/m^2 or 1000 W/m^2 with the latter representing a Leidenfrost, or film boiling, condition which is reached when the surface temperature is more than 200 K greater than the boiling point.

4.4 Fan Model

FSSIM has three models for evaluating the performance of a ventilation fan/blower. These are a constant pressure model, a quadratic model, and a user specified flow vs. pressure drop (head loss) model. For the constant pressure model, the user specifies a fixed pressure rise across the fan. This pressure is added to the momentum equations as a source term, the ΔP_j term in equation 4. For the quadratic model the user specifies the maximum volumetric flow, $\dot{V}_{full}$, at zero pressure drop across the fan and the pressure drop at which the flow rate becomes zero, $\Delta P_{shutoff}$:

$$\Delta P_j = \Delta P_{shutoff} - \left(\frac{\Delta P_j}{\dot{V}_{full}^{\ 2}} \right) \dot{V}_j^{\ 2} \tag{75}$$

At the beginning of each time step the volumetric flow through the fan is calculated. The fan pressure is solved for and used as the source term. To prevent oscillations in the fan source term the added pressure is relaxed between time steps using:

$$\Delta P_j^n = \beta \Delta P_j + (1-\beta) \Delta P_j^{n-1}, \tag{76}$$

where β is a relaxation factor, β=0.3.

For the user specified model the user inputs an array of pressure drop vs. volumetric flow rate. At each time step the current volumetric flow through the fan is determined from the prior time step velocity in the duct. A linear interpolation is performed to determine the next time step pressure which is then relaxed using Equation 76.

5.0 NOMENCLATURE

5.1 Roman

A	Area (m^2)
C_D	Discharge coefficient or droplet drag coefficient
c	Specific heat (J/kg-K)
c_p	Constant pressure specific heat (J/kg-K)
D	Diffusion coefficient (m^2/s)
d	Diameter
E	Energy (J)
F	Function or view factor
f	Friction factor
g	Gravitational acceleration (9.80665 m/s^2)
h	Enthalpy (J/kg) or heat transfer coefficient (W/m^2-K)
K	Form loss factor
k	Thermal conductivity (W/m-K)
L	Length (m)
M	Mass (kg)
mw	Molecular weight (kg/mol)
OD	Optical depth (m^{-1})
P	Pressure (Pa)
Pr	Prandtl number
q	Heat transfer rate (W)
R	Real gas constant (8.314472 N-m/mol-K)
Re	Reynolds number
r	Radius (m)
RTI	Response Time Index ($m^{1/2}s^{1/2}$)
Sc	Schmidt number
Sh	Sherwood number
T	Temperature (K)
t	Time (s)
V	Volume (m^3)
v	Velocity (m/s)
w	Suppression mass (kg).
X	Mole fraction (mol/mol) or x/z
x	Position (m)
Y	Mass fraction (kg/kg) or y/z
z	Vertical position (m)

5.2 Greek

α	Absorptivity (m^{-1})
β	Miscellaneous multiplier (i.e. relaxation factor)
Δ	Change in
ε	Emissivity or wall roughness (m)

ρ	Density (kg/m^3)
σ	Stefan-Boltzman constant ($5.6704x10^{-8}$ W/m^2-K^4) or direction function (1 or –1)
τ	Transmission factor or time constant (s)
χ_f	Radiative fraction

5.3 Superscripts

′	Per unit length (m^{-1})
″	Per unit area (m^{-2})
‴	Per unit volume (m^{-3})
in	Quantity is flowing inward to a node or compartment
n	Next time step
n+	Next time step guess
n-	Prior iteration
n-1	Prior time step
out	Quantity is flowing outward from node or compartment

5.4 Subscripts

act	Activation
air	Air
b	Boiling
c	Convection
d	Droplet, duct,or diameter
eq	Equivalent
equil	Evaluated at liquid-vapor equilibrium
evaporation	Results from evaporation of a liquid
ex	Exchange
f	Fire
fallout	Fallout of a liquid or solid aerosol from the gas phase
flood	Evaluated at the flooding criteria for vertical flow through an opening
full	Designates flowrate for fan or blower at zero head
gas	Gas
H_2O	Water
i	Compartment
j	Junction
k	Compartment
l	Liquid
loss	
mist	Mist droplet
n	Duct node
net	Sum of incoming and outgoing parameter
nozzle	Results from injection through a nozzle
outflow	Results from flow out of a compartment or node
pyro	Pyrolysis

r	Radiation
s	Soot
shutoff	Designates head at which fan/blower flow rate goes to zero
supp	Suppression system parameter
suppressed	Suppressed
v	Vapor
w	Surface

5.5 Overscripts

.	Time derivative (s^{-1})
~	Linearized value at next time step or modified net radiation term

6.0 REFERENCES

1. Adams, J., W. Brainerd, J. Martin, B. Smith, and J. Wagener. Fortran 95 Handbook Complete ISO/ANSI Reference. The MIT Press, Cambridge, MA, 1997.

2. Allelein, H. , et al. "Entwicklung und Verifikation eines Containment-Codesystems (COCOSYS) und eines deutsch-französischen Integralcodes (ASTEC)." GRS-A-2736, GRS-A-2737. Gesellschaft für Anlagen – und Reaktorsicherheit (GRS) mbH. 1999.

3. Back, G., E. Mack, M. Peatross, J. Scheffey, D. White, F. Williams, J. Farley, and D. Satterfield. "A Methodology for Predicting Fire and Smoke Spread Following a Weapon Hit." NRL Ltr Rpt Ser 6180/0014. Naval Research Laboratory. Washington, DC. 2003.

4. Cheremisinoff, N. Encyclopedia of Fluid Mechanics, Volume 3: Gas-Liquid Flows. Gulf Publishing Co., Houston, Texas, 1986.

5. Clift, R., J.Grace, and M. Weber. Bubbles, Drops and Particles. Academic Press. New York, NY. 1978.

6. Cooper, L. "Calculation of Flow Through a Horizontal Ceiling/Floor Vent." NISTIR 89-4052. National Institute of Standards and Technology. Gaithersburg, MD. 1989.

7. Crane Co. Flow of Fluids Through Valves, Fitting, and Pipe. Crane Technical Paper 410. Crane Co. Chicago, IL. 1988.

8. Dols, W., G. Walton, and K. Denton. "CONTAMW 1.0 User Manual: Mutizone Airflow and Contaminant Transport Analysis Software." NISTIR 6476. National Institute of Standards and Technology. Gaithersburg, MD. 2000.

9. Evans, D. "Sprinkler Fire Suppression Algorithm for HAZARD." NISTIR 5254. National Institute of Standards and Technology. Gaithersburg, MD. 1993.

10. Floyd, J., S. Hunt, F. Williams, and P. Tatem. "Fire + Smoke Simulator Version 1 (FSSIM) – Theory Manual." NRL. Washington, DC. 2004a.

11. Floyd, J., S. Hunt, F. Williams, and P. Tatem. "Fire + Smoke Simulator Version 1 (FSSIM) – User's Guide." NRL. Washington, DC. 2004b.

12. Floyd, J., F. Williams, and P. Tatem. "Fire + Smoke Simulator Version 1 (FSSIM) – Validation Report." NRL. Washington, DC. 2004c.

13. Forney, G. "Computing Radiative Heat Transfer Occurring in a Zone Fire Model." NISTIR 4709. National Institute of Standards and Technology. Gaithersburg, MD. 1991.

14. Gauntt, R., R. Cole, C. Erickson, R. Gido, R. Gasser, S. Rodriguez, M. Young. "MELCOR Computer Code Manuals: Reference Manuals Version 1.8.5." NUREG/CR-6119, Volume 2, Rev. 2. US Nuclear Regulatory Commission. Washington, DC. 2000.

15. George, T., L. Wiles, S. Claybrook, C. Wheeler, J. McElroy, and Singh, A. GOTHIC Containment Analysis Package Technical Manual Version 7.0. EPRI RP4444-1. Electric Power Research Institute, Inc. Palo Alto, CA. 2000a.

16. George, T., L. Wiles, S. Claybrook, C. Wheeler, J. McElroy, and Singh, A. "GOTHIC Containment Analysis Package User Manual Version 7.0." EPRI RP4444-1. Electric Power Research Institute, Inc. Palo Alto, CA. 2000b.

17. Haupt, T. Manual for FNM-GUI. 2004.

18. Hildebrand, F. Advanced Calculus for Applications. Prentice-Hall Inc. Englewood Cliffs, NJ. 1976.

19. Holman, J. Heat Transfer, 7th Edition. Mc-Graw Hill. New York, NY. 1990.

20. Jones, W., G. Forney, R. Peacock, and P. Reneke. "A Technical Reference for CFAST: An Engineering Tool for Estimating Fire Growth and Smoke Transport." NIST Technical Note 1431. National Institute of Standards and Technology. Gaithersburg, MD. 2000.

21. Karlsson, B. and J. Quintiere. Enclosure Fire Dynamics. CRC Press. Boca Raton, FL. 2000.

22. Klein-Heβling, et al. "COCOSYS V1.2 Manuals." GRS-P-3 (in preparation). Gesellschaft für Anlagen – und Reaktorsicherheit (GRS) mbH. 2000.

23. Mulholland, G. and C. Croarkin. "Specific Extinction Coefficient of Flame Generated Smoke." Fire and Materials. 24:227-230. 2000.

24. Schifiliti, R., B. Meacham, and R. Custer. "Design of Detector Systems". SFPE Handbook of Fire Protection Engineering, 3rd Edition. Philip DiNenno, et al. editors. Society of Fire Protection Engineers. Bethesda, Maryland. Section 4, Chapter 1. 2002.

25. Siegel, R., J. Howell. Thermal Radiation Heat Transfer, 4th ed. Taylor and Francis. New York, NY. 2001.

26. Spore, J., et al. "TRAC-M/FORTRAN 90 (Version 3.0) Theory Manual." LA-UR-00-910. Los Alamos National Laboratory. Los Alamos, NM. 2000.

27. Strauss, W. Partial Differential Equations: An Introduction. John Wiley & Sons. New York, NY. 1992.

28. Tien, C., K. Lee, and A. Stretton. "Radiation Heat Transfer". SFPE Handbook of Fire Protection Engineering, 3rd Edition. Philip DiNenno, et al. editors. Society of Fire Protection Engineers. Bethesda, Maryland. Section 1, Chapter 4. 2002.

29. USNRC. RELAP5/MOD3.3 Code Manual. United States Nuclear Regulatory Commission. Rockville, MD. 2001.

30. Wylen, G. and R. Sonntag. Fundamentals of Classical Thermodynamics: 3rd Edition. John Wiley & Sons. New York, NY. 1986.